

Angular distribution of photoelectrons in the above-threshold ionization of atomic hydrogen

Marek Trippenbach

Institute of Experimental Physics, Warsaw University, PL-00-681 Warsaw, ul. Hoża 69, Poland

Kazimierz Rzażewski

Institute for Theoretical Physics, Polish Academy of Sciences, PL-02-668 Warsaw, Aleja Lotników 32/46, Poland

Rainer Grobe

Fachbereich Physik, Universität Essen, D-43 Essen, West Germany

(Received 1 October 1987)

Using a multichannel version of the quantum-optical model of above-threshold ionization, we compute the angular distribution of photoelectrons for atomic hydrogen irradiated by a powerful linearly polarized laser pulse. We take into account the distortion of atomic continua by the presence of the strong laser. The distributions are peaked along the polarization direction. The results are in striking but qualitative agreement with the recent experiment of D. Feldmann *et al.* [*Z. Phys.* 6, 293 (1987)] for six- and four-photon ionization of hydrogen.

I. INTRODUCTION

Over the past several years, the experimental study of nonresonant multiphoton ionization of neutral atoms has led to the discovery of above-threshold ionization¹ (ATI). The phenomenon of ATI is an absorption of additional photons over the minimal number required for ionization. It manifests itself in an energy spectrum of the outgoing photoelectrons. This spectrum consists of a series of maxima spaced by the single-photon energy $\hbar\omega_L$ of the light used for ionization. The relative sizes of the peaks or the populations of the consecutive maxima depend on the intensity of the laser light, and in the region of $10^{12} \sim 10^{13}$ W/cm² become inverted. This means that a peak higher than the first one is most populated.

A number of theoretical ideas have been put forward to explain the striking features of ATI. Some of them had already been predicted in Ref. 2. It is possible that these ideas are complementary rather than conflicting and that more than one mechanism is at work in realistic situations.

Using a version of a high-intensity approximation,³ several authors² have computed partial cross sections for the multiphoton transition to higher ATI peaks. Their approach does not distinguish between different atoms, does not give a time dependence, and hence, leads to infinitely narrow peaks. Another idea is still based on the perturbation theory.^{4(a)} Consecutive peaks are the results of multiphoton transitions with the number of absorbed quanta growing from peak to peak. Hence, the *generalized partial* cross sections increase differently with the intensity of the incident light. At some point, inevitably, the second peak, and perhaps the third peak, becomes the most populated. In some papers⁵ quasiclassical expressions for the free-free matrix elements were used. The perturbative approach is in disagreement with some of the observations of the indices of nonlinearity.¹ Some authors⁶ suggest using a space-translation approach. A spe-

cial role would then be played by a static potential corresponding to an atomic Coulomb field averaged over the fast vibrations caused by the oscillating electric field and the bound states in this potential. The ground state of the atomic Hamiltonian can go over to the ground state of this averaged potential only under the condition of adiabatic switching. It is difficult, however, to reconcile this idea with the fact that some of the ATI experiments are performed with pulses as short as 500 fsec. Another interesting observation⁷ is that the photoelectrons in a typical ATI experiment are produced in the form of a charged ATI cloud, and hence, a Coulomb interaction between different charges (electrons and ions) should be accounted for. The space-charge effects tend to decrease the sizes of the lowest peaks. One should stress that some of the most recent experiments⁸ are believed to be done at such a low density that they are probably free of the space-charge effects, and nevertheless show peak switching. Some of the theoretical papers⁹ point to the importance of ponderomotive force. This is the force experienced by a charged particle traveling through an inhomogeneous electromagnetic field.¹⁰ This force acts on the photoelectrons while they are leaving the laser focus. Again some of the experimental works¹¹ claim a total absence of the ponderomotive-force effects. On the other hand, ponderomotive-force effects were clearly visible in the ATI experiments with ultrashort pulses.¹² Some properties of the peak envelope of the energy spectrum can be predicted on the basis of purely classical Monte-Carlo-type simulations.¹³ Such classical models, however, can never produce individual peaks.

Another line of thought is represented by a series of papers pointing to the saturation of free-free dipole transitions.¹⁴⁻¹⁶ The important ingredient of these papers is the identification of the subspace of essential states of the atom. Essential states are those which become populated during evolution. The total Hamiltonian is then restricted to the subspace of relevant states. A number of quali-

tative results were obtained using this framework, which are in rough agreement with the observed peak switching in the photoelectron spectra. The essential-states approach seems to be particularly attractive in application to the simplest possible system: a hydrogen atom. In this case one can perform the calculations without adjustable parameters.^{17,18} On this basis even a quantitative comparison between theoretical results and experimental data is possible. In the low-intensity limit such results can be checked against perturbation theory applied to hydrogen.^{4(b)}

The essential states in the model of ATI consist of the ground state and bands of continuum states labeled by their energy and angular-momentum quantum numbers. As emission and absorption of photons can only occur in the presence of accelerations, a relatively small number of partial waves should be present in the angular-momentum decomposition of the ATI peaks. The first results on this problem have recently been published¹⁹ and they indeed show that only roughly half of the angular momenta permitted by the dipole selection rule are present. The quantity measured directly is the angular distribution rather than the angular-momentum distribution. Moreover, the first angular distribution for ATI in atomic hydrogen has just been measured.²⁰ It is the purpose of this paper to present, for comparison, the *angular distributions* obtained within the extension of the model developed earlier,¹⁸ enriched by strong-field (sometimes called diagonal) corrections¹⁶ included by the method described in Ref. 21. In our model, the relevant states and the nonzero matrix elements of the Hamiltonian are shown in Fig. 1. The scheme is for a six-photon ionization by the powerful linearly polarized pulse of a Nd:YAG (yttrium aluminum garnet) laser. The six-photon bound-free transition is assumed to be entirely nonresonant. The corresponding matrix elements can be

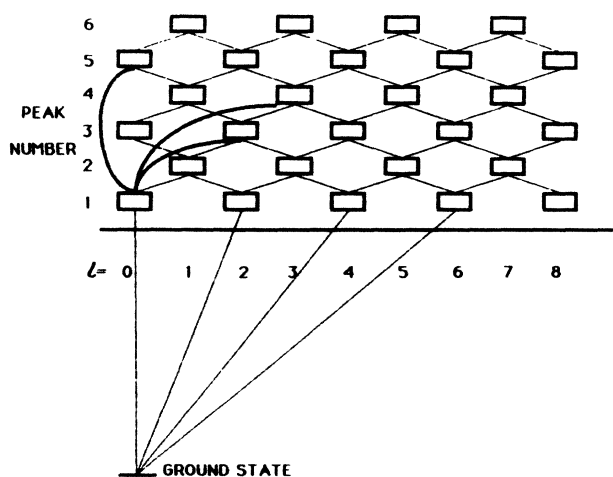


FIG. 1. Scheme of the essential states of our model calculations of six-photon ionization of hydrogen atom by linearly polarized light. Our initial state is the ground state. Bold lines within continuum represent some of the additional couplings introduced by the dressing of final atomic states, due to the presence of the strong laser field.

computed perturbatively.^{4(b)} For simplicity, we have used only one nonzero multiphoton matrix element linking the ground state with the $l=2$ band in the lowest continuum. It reproduces quite well the angular distribution of six-photon ionization of hydrogen obtained in Ref. 4(b) (we did the same for the four-photon case as well). Here we concentrate our attention on the transitions within the continuum.

We consider dipole free-free transitions. It is easy to check that the relevant matrix element of the momentum $\hat{\mathbf{p}}$ is a sum of two terms: $\langle \mathbf{q} | \hat{\mathbf{p}} | \mathbf{q}' \rangle = A(\mathbf{q}, \mathbf{q}') + B(\mathbf{q}, \mathbf{q}')$, of which the first one is a distribution (diagonal part) with support at $\mathbf{q}=\mathbf{q}'$ only, while the second (off-diagonal part) is a function not vanishing for $\mathbf{q} \neq \mathbf{q}'$. Note that for free motion ($|\mathbf{q}\rangle$ a plane wave), only the singular part remains and is equal to $q\delta^{(3)}(\mathbf{q}-\mathbf{q}')$. We use the free particle form of the diagonal part of the dipole matrix element even for Coulomb scattering states. It corresponds to the first Born approximation. The smooth part of the matrix element is responsible for real absorption and emission processes. It is analytically known²² for the hydrogen atom.

The method of elimination of the diagonal couplings is reviewed in Sec. II. Here we follow Ref. 21. In Sec. III we present the main results of our calculations. Section IV contains conclusions and perspectives for further improvement.

II. ESSENTIAL STATES MODEL OF ATI WITH DIAGONAL COUPLINGS

Here we consider the model of ATI described by the Hamiltonian (throughout the paper we will use atomic units)

$$H = H_0 + H_I, \quad H_I = \frac{\mathbf{p} \cdot \mathbf{A}}{c} \quad (2.1)$$

where the vector potential \mathbf{A} is given by

$$\mathbf{A} = \frac{\mathbf{E}}{\omega} \cos \omega t. \quad (2.2)$$

It represents linearly polarized light. Here, \mathbf{E} and ω are the laser field amplitude and frequency, respectively. H_0 is a Hamiltonian of an unperturbed hydrogen atom and the second term represents the semiclassical atom-field interaction. The term proportional to \mathbf{A}^2 is omitted since in the dipole approximation it merely shifts all energy levels by the same amount, without affecting the transitions. We expand the electron wave function $|\Psi(t)\rangle$ in terms of bound states $|k\rangle$ and continuum states $|\mathbf{p}\rangle$,

$$|\Psi(t)\rangle = \sum_k a_k(t) |k\rangle + \int a(\mathbf{p}, t) |\mathbf{p}\rangle d^3p, \quad (2.3)$$

and insert it into the Schrödinger equation. Within the continuum we have chosen the well-known basis of "outgoing Coulomb waves," which consists (in the asymptotic region) of a spherical outgoing wave and a distorted plane wave with well-defined momentum \mathbf{p} . Since the six- and four-photon ionization of hydrogen with sufficiently long interaction time is of interest in this paper, no intermediate resonance states play a role. Therefore, we introduce a direct effective coupling of $|0\rangle$ to continuum $|\mathbf{p}\rangle$ (ex-

pressed by the use of H_{eff}) neglecting the rest of the bound states. These simplifications lead to the following Schrödinger equation for expansion coefficients a_0 and $a(\mathbf{p}, t)$:

$$\begin{aligned} i\dot{a}_0 &= E_0 a_0 + \int d^3p \langle 0 | H_{\text{eff}} | \mathbf{p} \rangle a(\mathbf{p}, t), \\ i\dot{a}(\mathbf{p}, t) &= E_{\mathbf{p}} a(\mathbf{p}, t) + \langle \mathbf{p} | H_{\text{eff}} | 0 \rangle a_0 \\ &\quad + \int d^3p' \langle \mathbf{p} | H_I | \mathbf{p}' \rangle a(\mathbf{p}', t). \end{aligned} \quad (2.4)$$

The last term in the second equation describes transitions within the continuum. Since \mathbf{A} is a c -number operator, the matrix element $\langle \mathbf{p} | H_I | \mathbf{p}' \rangle$ is proportional to the matrix element of the $\hat{\mathbf{p}}$ operator between two Coulombic states $|\mathbf{p}\rangle$ and $|\mathbf{p}'\rangle$. As mentioned in Sec. I, this matrix element consists of two parts. The first part (we will call it off-diagonal since it does not disappear for $\mathbf{p} \neq \mathbf{p}'$) is a slowly varying function of both momenta and was found some 50 years ago by Gordon.²² As, however, $|\mathbf{p}\rangle$ consists (in the asymptotic region) of a (distorted) plane wave, the second term in $\langle \mathbf{p} | \hat{\mathbf{p}} | \mathbf{p}' \rangle$ should also exist, singular at a diagonal ($\mathbf{p} = \mathbf{p}'$). We can estimate the value of the latter, assuming for example that the electron is screened far from the interaction region (it means for this part we use plane waves instead of Coulombic states). Denoting the regular part by $g(\mathbf{p}, \mathbf{p}')$ we may write the decomposition as

$$\langle \mathbf{p} | H_I | \mathbf{p}' \rangle = g(\mathbf{p}, \mathbf{p}') \cos(\omega t) + \frac{\mathbf{p} \cdot \mathbf{E}}{c\omega} \delta(\mathbf{p} - \mathbf{p}') \cos(\omega t). \quad (2.5)$$

At this point we would like to make an important remark. The coefficients $a(\mathbf{p}, t)$ oscillate not only with their characteristic frequency $E_{\mathbf{p}}$. The term proportional to $a(\mathbf{p}, t) \cos(\omega t)$ in the second of Eqs. (2.4) introduces an extra oscillation to $a(\mathbf{p}, t)$ with all multiples of ω . In order to get rid of them and simplify the equations we substitute for $a(\mathbf{p}, t)$ with

$$\begin{aligned} i\dot{b}_0 &= \int d^3p b_{N_0}(\mathbf{p}, t) h(\mathbf{p}) J_0 \left[\frac{\mathbf{p} \cdot \mathbf{E}}{\omega^2 c} \right], \\ i\dot{b}_N(\mathbf{p}, t) &= \Delta_N b_N(\mathbf{p}, t) - \delta_{NN_0} b_0 J_0 \left[\frac{\mathbf{p} \cdot \mathbf{E}}{\omega^2 c} \right] h^*(\mathbf{p}) \\ &\quad + \sum_{N > N_0} \int d^3p' g(\mathbf{p}, \mathbf{p}') \left[J_{N-N'+1} \left[\frac{(\mathbf{p}-\mathbf{p}') \cdot \mathbf{E}}{\omega^2 c} \right] + J_{N-N'-1} \left[\frac{(\mathbf{p}-\mathbf{p}') \cdot \mathbf{E}}{\omega^2 c} \right] \right] b_N(\mathbf{p}', t), \end{aligned} \quad (2.10)$$

where $\Delta_N = E_N - E_0 - N\omega$ and the function $h(\mathbf{p})$ stands for the time-independent part of the matrix element of H_I between the ground state and the Coulombic continuum [$\langle 0 | H_I | \mathbf{p} \rangle = h(\mathbf{p}) \cos(\omega t)$]. As a result of a former assumption the ground state is coupled directly only to the

$$b(\mathbf{p}, t) = a(\mathbf{p}, t) \exp \left[-i \frac{\mathbf{p} \cdot \mathbf{E}}{c\omega} \sin(\omega t) \right]. \quad (2.6)$$

The time derivative of the exponent in (2.6), at the left-hand side of the second of Eqs. (2.4), cancels out the second part of the integral from $\langle \mathbf{p} | H_I | \mathbf{p}' \rangle$. Thus we can rewrite our basic set of equations in the following form [for convenience we also substitute $a_0 = b_0 \exp(iE_0 t)$]:

$$\begin{aligned} i\dot{b}_0 &= \int d^3p \langle \mathbf{p} | H_{\text{eff}} | 0 \rangle b(\mathbf{p}, t) \\ &\quad \times \exp \left[i \frac{\mathbf{p} \cdot \mathbf{E}}{\omega^2 c} \sin(\omega t) - iE_0 t \right], \\ i\dot{b}(\mathbf{p}, t) &= E_{\mathbf{p}} b(\mathbf{p}, t) + \int d^3p' g(\mathbf{p}, \mathbf{p}') b(\mathbf{p}', t) \cos(\omega t) \\ &\quad \times \exp \left[-i \frac{(\mathbf{p}-\mathbf{p}') \cdot \mathbf{E}}{\omega^2 c} \sin(\omega t) \right] \\ &\quad + b_0 \langle \mathbf{p} | H_{\text{eff}} | 0 \rangle \exp \left[-i \frac{\mathbf{p} \cdot \mathbf{E}}{\omega^2 c} \sin(\omega t) + iE_0 t \right]. \end{aligned} \quad (2.7)$$

In order to identify the essential states we perform a quasiharmonic expansion of all amplitudes:

$$b(\mathbf{p}, t) = \sum_{N > N_0} b_N(\mathbf{p}, t) \exp(iE_0 t - N\omega t). \quad (2.8)$$

Each $b_N(\mathbf{p}, t)$ is a slowly varying function of time and as a function of \mathbf{p} takes nonzero values only in the vicinity of $\mathbf{p}^2/2 = E_0 + N\omega$. Hence, $b_N(\mathbf{p}, t)$ is a probability amplitude of finding the electron in the N th ATI peak. The parameter N_0 is a minimal number of photons required for ionization.

To complete the Fourier expansion of Eqs. (2.7) we use a well-known formula²⁵

$$\exp[iz \sin(\omega t)] = \sum_{m=-\infty}^{+\infty} J_m(z) e^{im\omega t}. \quad (2.9)$$

Now we compare amplitudes of the terms which oscillate with the same frequency on both sides of our set of Schrödinger equations (2.7). This is a form of the rotating-wave approximation (RWA)

first energy band in the continuum, but the introduction of $b_N(\mathbf{p}, t)$ leads to the emergence of couplings between energy bands in the strong laser field. In the present paper we focus our attention on the hydrogen atom, for which the function $g(\mathbf{p}, \mathbf{p}')$ is known²² and the function

$h(\mathbf{p})$ can be computed with the help of perturbation methods.^{4(b),17} Having in mind further use of the essential-states approach²³ for the reduction of the integrodifferential equation to the rate equation, we pass at this point from the momentum ($|\mathbf{p}\rangle$) basis to the energy-angular-momentum ($|\mathbf{E}, l, m\rangle$) basis,²⁴

$$|\mathbf{p}\rangle = \sum_{l=0}^{\infty} \sum_{m=-l}^l \frac{1}{2\pi |\mathbf{p}|} e^{-2i\delta_l} Y_{l,m}(\theta, \phi) |\mathbf{E}, l, m\rangle. \quad (2.11)$$

Only states with $m=0$ contribute to the dynamics due to the dipole selection rules and the spherical symmetry of the ground state.

The Coulombic phases are given by the well-known formula²⁴

$$\gamma_l = e^{-2i\delta_l} = \frac{\Gamma\left[l+1+\frac{i}{p}\right]}{\Gamma\left[l+1-\frac{i}{p}\right]}. \quad (2.12)$$

Due to the cylindrical symmetry of the atom-plus-field system, $b_N(\mathbf{p}, t)$ can be expanded into Legendre polynomials,

$$K_N^l(E) = \sum_{l'=0}^{\infty} h_{l'}(E) \gamma_{l'} G_N^{l,l'}(E) \delta_{NN_0}, \quad (2.17)$$

$$L_{N,N'}^{l,l'}(E, E') = i\sqrt{l}(N-N') \sum_{j=0}^{\infty} \sum_{s=\pm 1} \gamma^{j*} \gamma^{j+s} W_{j,j+s}(E, E') \sum_{M=-\infty}^{+\infty} \sum_{r=\pm 1} G_M^{l,l'}(E) G_{M+N-N'+r}^{l,l'}(E'), \quad (2.18)$$

where $W_{j,l}(E, E')$ denotes matrix elements of \hat{r} between $|E, l\rangle, |E', l'\rangle$.

In deriving the final set of equations (2.16) we used the addition theorem for the Bessel functions,²⁵

$$J_k(u-v) = \sum_{s=-\infty}^{+\infty} J_{s+k}(u) J_s(v). \quad (2.19)$$

Under the usual assumption of flat continua (i.e., neglecting the energy dependence of the couplings), our final set of equations may be reduced to the set of rate equations following the steps worked out in Ref. 23.

Note that in contrast to the model calculations of Ref. 18, where diagonal couplings were neglected, the present version of the model contains couplings between all essential states continua and the couplings [(2.17) and (2.18)] are highly nonlinear functions of the laser intensity.

III. ANGULAR DISTRIBUTIONS

We notice that the intensity of the laser light enters the continuum-continuum couplings [(2.17) and (2.18)] through the dimensionless parameter $\alpha = \mathbf{p} \cdot \mathbf{E} / \omega^2 c$, which is an argument of the Bessel functions. This parameter also plays an important role in the study of collisions in the presence of the laser field.²⁶ It is evident that these

$$b_N(\mathbf{p}, t) = \sum_{l=0}^{\infty} b_N^l(E, t) Y_{l,0}(\theta), \quad (2.13)$$

where $b_N^l(E, t)$ depends only on the energy, the whole angular dependence being shifted to $Y_{l,0}$.

The first of our Eqs. (2.10) takes the following form in the angular-momentum basis:

$$i\dot{b}_0 = \sum_{l,l'} \int dE h_l(E) \gamma_l G_0^{l,l'}(E) b_{N_0}^l(E, t), \quad (2.14)$$

where

$$G_k^{l,l'}(E) = \int d\Omega Y_{l,0}(\theta) J_k \left[\frac{\mathbf{p} \cdot \mathbf{E}}{\omega^2 c} \right] Y_{l',0}(\theta). \quad (2.15)$$

Now, decomposing the second of our Eqs. (2.10) into Legendre polynomials we obtain a set of equations

$$\begin{aligned} i\dot{b}_0 &= \sum_{l=0}^{\infty} \sum_{N \geq N_0} \int dE K_N^l(E) b_N^l(E, t), \\ i\dot{b}_N^l(E, t) &= \Delta_N b_N^l(E, t) + K_N^l(E) b_0 \\ &+ \sum_{N' > N_0} \sum_{l'=0}^{\infty} \int dE' L_{N,N'}^{l,l'}(E, E') b_{N'}^{l'}(E', t). \end{aligned} \quad (2.16)$$

In this equation the couplings take the following form:

two processes have a lot in common. For decreasing laser intensity the parameter α tends to zero, and, as one can easily check on our final set of Eqs. (2.16), they reproduce exactly the model of Ref. 18 which contains only off-diagonal couplings.

It is a main purpose of our paper to present angular distributions of outgoing electrons resulting from our model. Through the reduction of the Eqs. (2.16) to the rate equations, we finally calculate a set of amplitudes f_N^l . They may be interpreted as the probability amplitudes of finding the outgoing electron with angular momentum l within the N th peak.

The vector f_N^l is computed by a simple matrix inversion

$$f_N^l = \sum_{N'} \sum_{l'} \left[\frac{1}{1+i\pi L} \right]_{NN'}^{ll'} K_{N'}^{l'}, \quad (3.1)$$

where the matrix L is composed of free-free couplings (2.17).

The angular distribution in the N th peak, $W_N(\theta)$, is then defined by

$$W_N(\theta) = \left| \sum_l f_N^l Y_{l,0}(\theta) \right|^2. \quad (3.2)$$

Note that the Coulombic phases (2.12) are already included in the definition of amplitudes f_N^l .

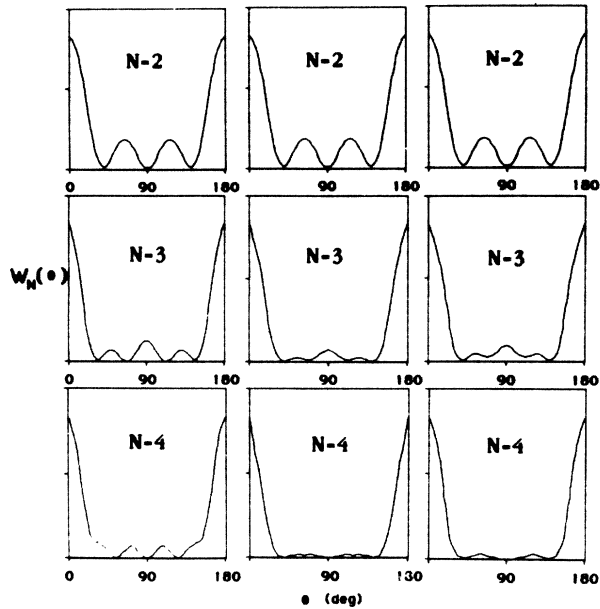


FIG. 2. Stabilization of angular distribution for six-photon ionization of hydrogen with increasing number of couplings included. The assumed intensity of the light is 5×10^{-4} a.u. ($\sim 1.75 \times 10^{13}$ W/cm²). Note that higher peaks demand more terms in the expansion.

In Fig. 1 we show the scheme of the relevant states and their couplings in our model calculations of six-photon ionization of hydrogen. We stress that all the bands of the given peak are coupled to all the bands of the other peaks. As the full solution of our problem requires a substantial numerical effort, we simplify the task by making power expansion of all the couplings L [see (2.18)] in parameter α . We observe that the power of the lowest-order term in the expansion increases with the distance between the bands. We therefore can set up a method of consecutive approximations. Following our procedure we increase step by step a number of coupled energy bands. With increasing order of this expansion more distant states become coupled. To estimate the population and angular distribution of a certain peak one has to include as many couplings as are necessary to achieve a stable result.

The stabilization mechanism is illustrated in Fig. 2 and

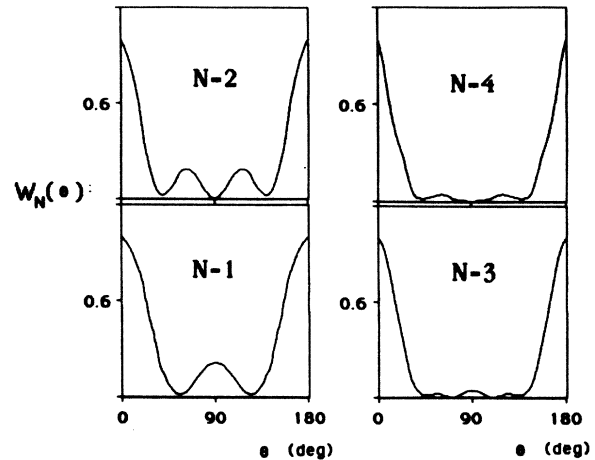


FIG. 3. Angular distribution of photoelectrons in the first five peaks in six-photon ionization of hydrogen by linearly polarized frequency doubled Nd:YAG laser light. The assumed intensity of the light is 5×10^{-4} a.u. ($\sim 1.75 \times 10^{13}$ W/cm²).

Table I. Three series of graphs present angular distributions in the second, third, and fourth peak, as obtained from our model with single, double, and triple transitions included. Note that higher peaks demand more terms in the expansion. Of course it is more difficult to reach stability for higher laser intensities. The stabilization of the energy distribution is illustrated in Table I. There is a close correspondence between the stabilization of both quantities.

The final results for the angular distribution of six-photon ionization are presented in Fig. 3. The results are in direct correspondence with the recent experiment performed in Ref. 20. In fact we have chosen the laser intensity of 5×10^{-4} a.u. to match the peak ratio of the experiment. The population of the second peak was about 10% of the first one. Even though for the chosen intensity the size of the couplings decreases with the distance between the continua, an increasing number of them must be included to obtain reliable angular distributions of photoelectrons in higher peaks. Due to numerical limitations, we restricted ourselves to the analyses of the five lowest peaks. There is a substantial wiggling in the lowest peaks. As we go up, the distribution develops clear forward and backward maxima. Of course one can interpret

TABLE I. Stabilization of the energy spectrum with increasing number of couplings included. We quote results for six-photon ionization of hydrogen. Laser intensity is 10^{-6} a.u.

Peak number	Number of couplings	Number of couplings				
		1	2 ($\times 10^{-3}$)	3 ($\times 10^{-6}$)	4 ($\times 10^{-9}$)	5 ($\times 10^{-12}$)
$N=1$	1.000	1.000	0.452	0.144	0.068	0.049
$N=2$	1.000	1.000	0.452	0.374	0.236	0.445
$N=3$	1.000	1.000	0.452	0.374	0.361	0.587
$N=4$	1.000	1.000	0.452	0.374	0.361	0.705
$N=5$	1.000	1.000	0.452	0.374	0.361	0.705

the maxima of the angular distribution classically: They result from the force exerted on the electron by the electric field of the laser light. Similar peaks appear in purely classical numerical simulations.¹³ All of these are in striking though qualitative agreement with the experimental results of Ref. 20. In particular, our results are consistently smoother between the forward and backward maxima than the experimental ones.

In Fig. 4 the corresponding results for the four-photon ionization are shown. Once again the only nonzero bound-free matrix element is that linking the ground state with $l=2$ band in the lowest continuum. At the intensity of the experiment the flow of the population to the higher peaks is small and the angular distribution of the first peak is fully determined by this choice. So far only the first two peaks were analyzed experimentally in this case.

IV. CONCLUSIONS

The multichannel quantum optical model of ATI predicts a qualitatively correct angular distribution. The angular distribution (unlike the energy distribution) is surprisingly sensitive to the distortion of the final continuous states due to the presence of the strong electromagnetic field. This distortion is represented by the diagonal parts of the free-free dipole matrix elements. The importance of such terms has been stressed in Ref. 16.

There is ample room for improvements of the present model.

- (1) The diagonal elements of the dipole matrix elements are used in the first Born approximation.
- (2) The temporal and spatial shape of the laser pulse is ignored.
- (3) Laser intensity fluctuations are omitted.
- (4) The assumption of completely flat continua, necessary for the reduction of our equations to the rate equa-

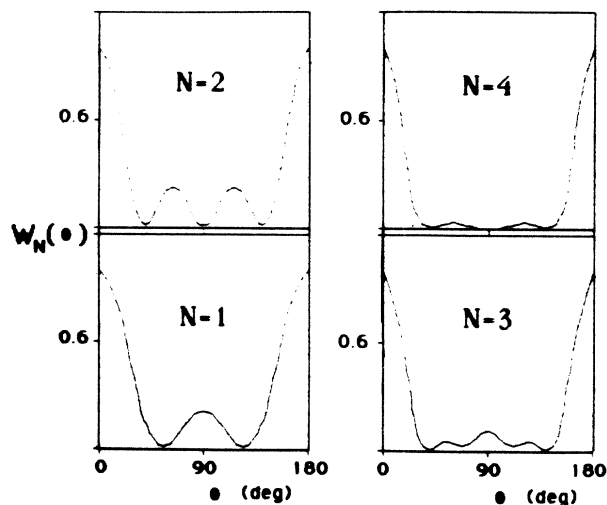


FIG. 4. Same as Fig. 3 but for the four-photon ionization by the frequency tripled Nd:YAG laser.

tions, is not perfect.

One should also stress that the first experimental results of Ref. 20 are not very accurate and further improvement is necessary to discriminate between different theoretical models of ATI.

ACKNOWLEDGMENTS

Two of us (M.T. and K.R.) would like to acknowledge the support of the Polish Government Grant Nos. CPBP 01.06 and CPBP 01.07. This work is a result of an ongoing cooperation program between Fachbereich Physik of Universität Essen and the Institute for Theoretical Physics of the Polish Academy of Sciences.

¹P. Agostini, F. Fabre, G. Mainfray, G. Petite, and N. Rahman, *Phys. Rev. Lett.* **42**, 1127 (1979); P. Kruit, J. Kimman, and M. van der Wiel, *J. Phys. B* **14**, L597 (1981); F. Fabre, G. Petite, P. Agostini, and M. Clement, *J. Phys. B* **15**, 1353 (1982).

²A. I. Nikishov and V. I. Ritus, *Zh. Eksp. Teor. Fiz.* **50**, 255 (1966) [*Sov. Phys.—JETP* **23**, 168 (1966)]; F. H. M. Faisal, *J. Phys. B* **6**, L89 (1973), H. R. Reiss, *Phys. Rev. A* **22**, 1786 (1980).

³L. V. Keldysh, *Zh. Eksp. Teor. Fiz.* **47**, 1945 (1964) [*Sov. Phys.—JETP* **20**, 1307 (1965)].

⁴(a) Y. Gontier and M. Trahin, *Phys. Rev.* **172**, 83 (1968); *Phys. Rev. A* **4**, 1896 (1971); **7**, 2069 (1973); *J. Phys. B* **13**, 4383 (1980); (b) Y. Gontier, N. K. Rahman, and M. Trahin, *J. Phys. B* **8**, L179 (1975); *Phys. Rev. A* **34**, 1112 (1986).

⁵N. B. Delone, S. P. Goreslavski, and V. P. Krainov, *J. Phys. B* **16**, 2369 (1983); I. Ya. Bersons, *Habilitation*, Latvian Academy of Sciences, Riga.

⁶M. Pont and M. Gavrilu, *Phys. Lett. A* **123**, 469 (1987).

⁷M. Crance, *J. Phys. B* **19**, L267 (1986); **19**, L671 (1986).

⁸F. Yergeau, G. Petite, and P. Agostini, *J. Phys. B* **19**, L663 (1986).

⁹O. H. Muller, A. Tip, and M. van der Wiel, *J. Phys. B* **16**, L679 (1983); M. H. Mittleman, *Prog. Quantum Electron.* **8**, 165 (1984); S. I. Chu and J. Cooper, *Phys. Rev. A* **32**, 2769 (1985); L. Pan, L. Armstrong, Jr., and J. H. Eberly, *J. Opt. Soc. Am. B* **3**, 1319 (1986).

¹⁰R. R. Freeman, T. J. McIlrath, P. H. Bucksbaum, and M. Bashkansky, *Phys. Rev. Lett.* **56**, 2590 (1986).

¹¹L. A. Lompre, A. L'Huillier, G. Mainfray, and C. Manus, *J. Opt. Soc. Am. B* **2**, 1906 (1985).

¹²R. R. Freeman, T. J. McIlrath, P. H. Bucksbaum, and M. Bashkansky, *Phys. Rev. Lett.* **57**, 3156 (1986); P. H. Bucksbaum, R. R. Freeman, M. Bashkansky, and T. J. McIlrath, *J. Opt. Soc. Am. B* **4**, 760 (1987); R. R. Freeman, P. H. Bucksbaum, H. Milchberg, S. Darack, D. Schumacher, and M. E. Geusic (unpublished).

¹³J. Grochmalicki, J. Mostowski, and M. Trippenbach (unpublished).

¹⁴Z. Białyńska-Birula, *J. Phys. B* **17**, 3091 (1984).

- ¹⁵M. Edwards, L. Pan, and L. Armstrong, Jr., *J. Phys. B* **17**, L515 (1984); **18**, 1927 (1985); Z. Deng and J. H. Eberly, *Phys. Rev. Lett.* **53**, 1810 (1984); *J. Opt. Soc. Am. B* **2**, 486 (1985).
- ¹⁶M. Lewenstein, J. Mostowski, and M. Trippenbach, *J. Phys. B* **18**, L461 (1985); J. Grochmalicki, J. R. Kuklinski, and M. Lewenstein, *ibid.* **19**, 3649 (1986).
- ¹⁷The hydrogen atom was always a test case for the theory of multiphoton processes. Compare with W. Zernik, *Phys. Rev.* **135**, 51 (1964); H. B. Bebb and A. Gold, *ibid.* **149**, 25 (1966); F. T. Chan and C. L. Tang, *ibid.* **185**, 42 (1969); S. Klarsfeld and A. Maquet, *Phys. Lett.* **73A**, 100 (1979); G. Laplanche, A. Durrieu, Y. Flank, M. Jaouen, and A. Rachman, *J. Phys. B* **9**, 1263 (1976); see also Ref. 5.
- ¹⁸K. Rzażewski and R. Grobe, *Phys. Rev. Lett.* **54**, 1729 (1985); *Phys. Rev. A* **33**, 1855 (1986).
- ¹⁹H. J. Humpert, H. Schwier, R. Hippler, and H. O. Lutz, *Phys. Rev. A* **32**, 3787 (1985).
- ²⁰D. Feldmann, B. Wolff, M. Wemhoner, and K. H. Welge, *Z. Phys.* **6**, 293 (1987).
- ²¹M. Trippenbach, *J. Opt. Soc. Am. B* **4**, 1429 (1987).
- ²²W. Gordon, *Ann. Phys. (N.Y.)* **2**, 1031 (1929).
- ²³M. Crance and M. Aymar, *J. Phys. B* **13**, L421 (1980).
- ²⁴See, for instance, L. D. Landau and M. Lifshitz, *Quantum Mechanics* (Pergamon, New York, 1958), Vol. 3.
- ²⁵*Handbook of Mathematical Functions*, edited by M. Abramowitz and I. A. Stegun (Dover, New York, 1970).
- ²⁶F. V. Bunkin and M. V. Fedorov, *Zh. Eksp. Teor. Fiz.* **48**, 1341 (1965) [*Sov. Phys.—JETP* **21**, 896 (1965)]; N. M. Kroll and K. M. Watson, *Phys. Rev. A* **8**, 804 (1973).